Iran Red Crescent Med J. 2017 March; 19(3):e41336. doi: 10.5812/ircmj.41336.

Published online 2016 November 26. **Research Article**

Feature Extraction and Classification of Breast Tumors Using Chaos and Fractal Analysis on Dynamic Magnetic Resonance Imaging

Mahyar Nirouei,[1] Majid Pouladian,[2,*] Parviz Abdolmaleki,[3] and Shahram Akhlaghpour[4]

[1]Department of Medical Radiation Engineering, Science and Research Branch, Islamic Azad University, Tehran, IR Iran
[2]Department of Biomedical Engineering, Science and Research Branch, Islamic Azad University, Tehran, IR Iran
[3]Department of Bio-Physics, Faculty of Science, Tarbiat Modares University, Tehran, IR Iran
[4]Pardisnoor Medical Imaging Center, Tehran, IR Iran

[*]*Corresponding author*: Majid Pouladian, Department of Biomedical Engineering, Science and Research Branch, Islamic Azad University, Tehran, IR Iran. E-mail: pouladian@srbiau.ac.ir

Received 2016 August 26; **Revised** 2016 October 29; **Accepted** 2016 November 14.

Abstract

Background: Breast cancer is one of the leading causes of death in the world. Early diagnosis of breast cancer can reduce the rate of mortality of this type of cancer. An increasing number of reports have confirmed the excellent sensitivity of dynamic contrast enhanced magnetic resonance imaging (DCE-MRI). Despite the excellent sensitivity of DCE-MRI, there is still some difficulty in the prediction of malignancy in these patients because of the lack of the optimum guidelines for the interpretation of breast magnetic resonance (MR) studies as well as the reported overlap in T1 and T2 relaxation times.
Objectives: The aim of this study was to extract significant features from MRI images of the breast using chaos, fractal and time series analysis and to classify breast tumors into malignant and benign using the calculated features.
Methods: In this research, we utilized the chaos theory and fractal analysis in the interpretation of breast tumors on DCE-MRI. This cross-sectional study was done at Pardisnoor imaging center during years 2015 and 2016 in Iran. Our sample size was 18 mass lesions, which were randomly selected among patients with BIRAD 3 and BIRAD 4 classification by the expert radiologist. The analysis was performed after injecting patients with a contrast agent and 18 mass lesions were extracted from dynamic MR images. After preprocessing and segmentation stages, time series of the tumor was generated for each MR image. The largest Lyapunov exponent (LLE) and statistical parameters for each mass lesion were extracted. Also, fractal analysis was utilized to extract meaningful features from mass contour to evaluate the roughness of tumor margin.
Results: We found that the value of LLE in malignant tumors was higher than benign mass lesions. The obtained results demonstrated that chaos and time series features, such as LLE and non-circularity of the tumor, were the best parameters among all features.
Conclusions: The extracted descriptors can improve the performance of classifiers in the early detection of breast cancer. Significant shape features can also help radiologists increase diagnosis accuracy in classification of suspicious breast masses.

Keywords: Chaos Analysis, Feature Extraction, Lyapunov Exponents, Breast Cancer, Dynamic MRI

1. Background

Breast cancer is a universal health problem in the female population. Although mammography remains the most sensitive diagnostic procedure for the early detection of breast cancer, the low specificity of this method can lead to unnecessary breast biopsies. To grapple with this problem, magnetic resonance imaging (MRI) methods have been investigated especially in females with dense breast tissue. Injection of a contrast agent such as Gd-DTPA can lead to higher sensitivity and specificity of MRI for the early diagnosis of breast cancer (1).

The characteristics of malignant tumors such as spatial heterogeneity, chaotic structures and fragile vessels, are suitable to be studied by dynamic contrast enhanced magnetic resonance imaging (DCE-MRI) (2). Although DCE-MRI is a powerful technique for visualizing angiogenesis, irregularity and chaotic features of breast tumors, there are no papers with a focus on the chaotic behavior of breast tumors using dynamic MRI. The low resolution of MRI can be one of the main limitations, which can reduce its applications in these studies. On the other hand, an increasing number of reports have confirmed the excellent potential of chaos theory for analyzing different types of cancer using high resolution imaging techniques.

Lee et al. used time-intensity curve shape based on a three-time-points (3TP) solution, which generates a color map allowing kinetic analysis from the intensity levels and can classify malignant and benign lesions (3).

Recent studies have shown that fractal analysis can be helpful for quantifying chaotic and complicated pathologic architecture of tumors (4). Fractal dimension has shown good performance in classification of cancers, especially in high-resolution imaging techniques as a reproducible measure of complexity (5, 6). Researchers are well

informed of the advances in chaos theory and nonlinear dynamics and their clinical applications in the field of medicine (7). Etehadtavakol et al. used nonlinear dynamics utilizing Lyapunov exponents (LE) in breast thermograms to identify abnormal lesions of the breast (8). Abe et al. showed an application of the largest Lyapunov exponent (LLE) for characterizing brain structural information on MRI control and mental disorders (9). It was recently reported that cell shape, sub-cellular sizes and spatial intracellular distribution could control how molecules interact to produce a cellular behavior (10). The behavior of malignant and benign cells and their spatial distribution can affect the shape, margin and texture of malignant and benign tumors in the larger scale. Finding a way to mathematically analyze tumor margin and its texture in the large scale can improve the diagnosis accuracy in classifying malignant and benign tumors. Although it would be better to study molecular and cellular behavior of tumors, the resolution of medical imaging techniques is a major limitation of this study. Therefore, we need to study footprints of tumor cellular distribution in different scales using fractal and chaos theory as mentioned before. Badas et al. presented 3D finite time Lyapunov exponent evolution inside a left ventricle in-vitro model mimicking physiological human conditions (11). Rangayyan et al. used the ruler method and the box-counting method for estimation of fractal dimension from contours of breast masses (12). Beheshti et al. showed that extracting fractal features from contours of masses on different types of breast density mammograms was able to successfully classify breast tumors (13). The success of chaos analysis in biomedical research persuades us to use this method in the early detection of breast cancer as an important unsolved health problem. This is the first research on the application of chaos in breast cancer diagnosis on DCE-MRI.

2. Objectives

The aim of this study was to look for possible differences between malignant and benign breast masses using fractal analysis, nonlinear chaotic dynamical systems and time series of tumor contour on DCE-MRI. We extracted several chaotic features to quantify the degree of chaos in breast tumor margins. Also we utilized fractal analysis in extracting fractal features to analyze the texture of breast tumors and make comparisons with chaos features. These features can improve the efficiency of classifiers to develop computer-aided diagnosis models and decrease misclassification rate of breast cancer diagnosis.

3. Methods

3.1. Database

Our study group consisted of 13 patients whose ages ranged from 18 to 57 years (mean 40.2 years). Our sample size was 18 mass lesions that consisted of nine malignant lesions and nine benign entities, which were randomly selected among patients with BIRAD 3 and BIRAD 4 classification by the expert radiologist. The inclusion criteria consisted of there being at least one mass (with BIRAD 3 or BIRAD 4 classification) in the subject's breast and the availability of patient's MR images with standard imaging protocol. On the other hand, pregnant patients and allergic patients to gadolinium contrast agent were excluded from our study. We did not have any missing value in our database. Informed consent was obtained from all patients or their relatives. All patients underwent a surgical biopsy. Their basic information is presented in Table 1.

3.2. Data Acquisition

Magnetic resonance imaging was performed at the Pardisnoor imaging center during years 2015 and 2016, using a calibrated 1.5 Tesla ACHIEVA Philips MR scanner in the prone position with a specific breast coil. The dynamic study was performed after injection of 0.1 (mmol/kg) of gadopentetate dimeglumine. The DCE portion of the MRI was based on a standard clinical protocol that consisted of a series of T1 weighted, fat-suppressed, three-dimensional gradient echo acquisitions in the axial plane with the following parameters: repetition time, 4.9 - 5.4 ms; echo time, 2 - 2.5 ms; 10° flip angle, field of view, 240 $\times$ 240 (mm^2), voxel size, 1 $\times$ 1 $\times$ 1 (mm^3), matrix, 320 $\times$ 320 and temporal resolution of 80 - 90 seconds (14).

3.3. Time Series Extraction

The extracted time series from tumor margin, which can be considered as a nonlinear system contains valuable diagnostic information. To capture this information, conventional methods, such as Fourier transform, were not successful due to the nonlinearity of system dynamics. Chaos analysis is a suitable alternative to describe nonlinear and complex systems. In this paper, we considered breast tumors as a nonlinear complex system, which can be described by a strange attractor in phase space (PS). The time evolution of these observables in the state-space establishes a trajectory (8). We didn't have enough information about the dynamics of the system. We had only one TS measurement (8). In such case, it is not possible to find the exact PS of the system. Therefore, a pseudo-PS may still be constructed. This pseudo-PS is called the reconstructed phase space (RPS) (8). In this research, Time Delay Embedding (TDE) method was used for PS reconstruction.

Table 1. Lesion Characteristics

Lesion Number	Gender	Pathology	BIRAD Classification	Age	Type
1	Female	Benign	4b	33	Fibroadenoma
2	Female	Benign	4	35	Fibroadenoma
3	Female	Benign	4b	18	Intraductal Papilloma
4	Female	Benign	4	42	Intraductal Papilloma
5	Female	Benign	4b	37	Invasive Ductal Carcinoma
6	Female	Benign	4	42	Intraductal Papilloma
7	Female	Benign	4a	57	Fibroadenoma
8	Female	Benign	4a	40	Intraductal Papilloma
9	Female	Benign	4	36	Fibroadenoma
10	Female	Malignant	4b	37	Invasive Ductal Carcinoma
11	Female	Malignant	4b	37	Invasive Ductal Carcinoma
12	Female	Malignant	4b	43	Invasive Ductal Carcinoma
13	Female	Malignant	4b	43	Invasive Ductal Carcinoma
14	Female	Malignant	4a	53	Invasive Ductal Carcinoma
15	Female	Malignant	3	53	Invasive Ductal Carcinoma
16	Female	Malignant	4b	43	Invasive Ductal Carcinoma
17	Female	Malignant	4c	36	Invasive Ductal Carcinoma
18	Female	Malignant	4b	38	Invasive Ductal Carcinoma

In order to extract the time series from tumor boundary, we selected the best part of MR images for each tumor. The center of gravity of the tumor was calculated in each MR image and tumor margin was traced utilizing Fuzzy C-Mean (FCM) segmentation method. The FCM is a fast and easy to use segmentation method, which can be suitable to segment ill-defined breast tumors from the background (15, 16). Then, the distance of each pixel on the tumor margin from the center of gravity was measured and used for extracting the time series for all breast lesions. Using this method, we converted the tumor shape into a time series. Figure 1 shows a typical MR image after pre-processing and filtering by the median filter. Figure 2 shows the segmented tumor and its depicted contour using Fuzzy C-Mean segmentation algorithm and "bwtraceboundary" in Matlab.

Figure 3 shows time series extracted from the tumor contour of Figure 2. We extracted chaos features from the time series by calculating the LLE of the extracted time series. Figures 4 and 5 demonstrate the extracted benign and malignant mass lesions, respectively, and their depicted contour using the FCM method. Also, the centers of mass of all tumors were shown in these images.

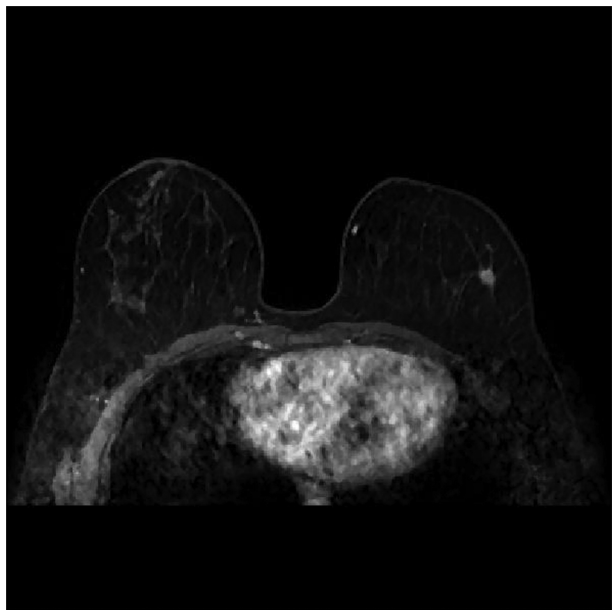

Figure 1. Filtered Image Using Median Filter

3.4. Embedding Dimension and Time Delay

We utilized time delay embedding to reconstruct the phase space. A chaotic time series can be embedded into

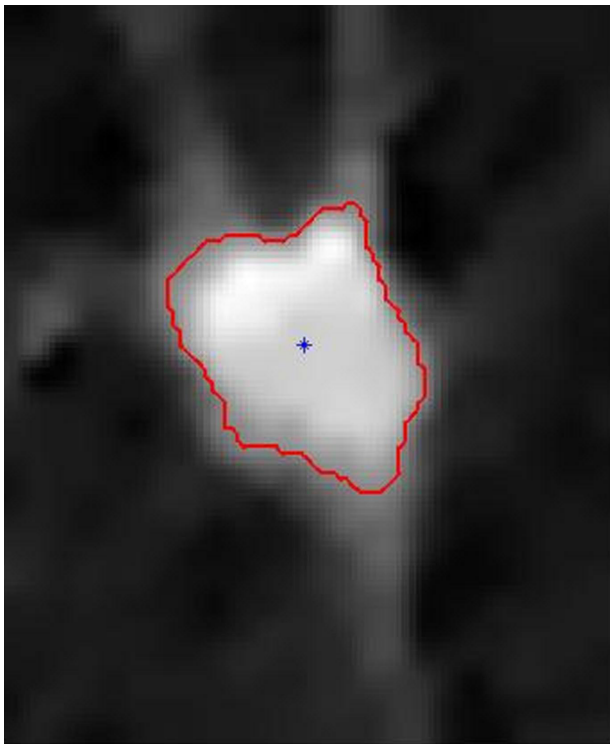

Figure 2. Segmented Tumor Using Fuzzy C-Mean Method

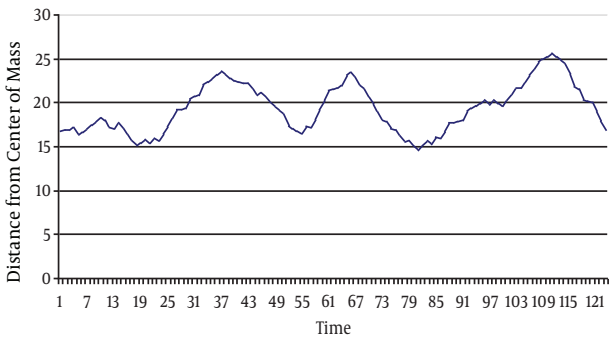

Figure 3. Time Series Extracted From Tumor Contour

an RPS with an embedding dimension m and a time delay J. In the TDE method, two parameters are necessary to be selected and optimized, the embedding dimension, m, and the time delay J. These parameters should be optimal enough due to their impact on calculating the LEs (8). The inherent system dimension was considered as d. According to Takens' theorem, if the system dimension is d, we can establish an RPS that is equivalent to the original PS by embedding with a dimension m (greater than 2d + 1) (17).

In order to be able to identify an attractor, the time delay should be selected optimally. Many methods have been proposed for selecting an optimal time delay but it is still not possible to apply a unique method for all types of data (9). We used the autocorrelation indicator for time delay estimation.

3.5. Calculation of Largest Lyapunov Exponent

To calculate the LLE, we considered a discrete system with a 1-D map $x_{k+1} = f(xk)$, which evolves when it is started at two initial conditions of x_0 and $(x_0 + \varepsilon_0)$ (10, 11). The parameter ε_0 requires a small value to show the two initial states are very close to each other. The Lyapunov exponent is defined when the two trajectories are diverged by a distance ε_n after n iterations, as follows (Equation 1).

$$|\epsilon_n| \approx |\epsilon_0| e^{n\lambda} \quad (1)$$

Where λ is the Lyapunov exponent (10).

A practical numerical technique for calculating the LLE is the method developed by Rosenstein et al. (9). Due to its robustness to time delay and embedding dimension changes, this well-known method was applied in this research to calculate the LLE of the MRI-based time series (18). We changed embedding dimension (m) in our program from 2 to 5 and the best value was m = 2. The autocorrelation method was used for time delay estimation. The implementation of this method is easy because it utilizes a simple measure of exponential divergence (9, 18).

3.6. Fractal Analysis

The concept of fractals was proposed by Mandelbrot to describe objects with irregular structures (13). For quantifying the complexity and self-similarity of the structure of an object, a measure known as the fractal dimension (FD) can be utilized (12). A self-similar structure was considered, which consists of a number of self-similar pieces at the reduction factor 1/s (12). FD can be defined as follows (Equation 2):

$$\alpha = \frac{1}{S^{FD}} \quad (2)$$

Then, we have (Equation 3):

$$FD = \frac{\log(\alpha)}{\log\left(\frac{1}{s}\right)} \quad (3)$$

The most commonly used method for estimating FD is the box-counting method. We used this method for calculation of fractal dimension and other fractal parameters.

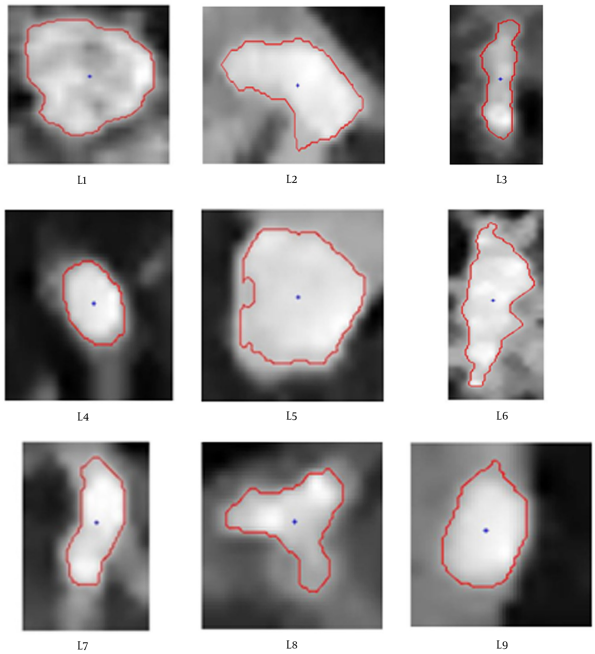

Figure 4. Extracted Benign Mass Lesions and Their Depicted Contour Using Fuzzy C-Mean Segmentation Method

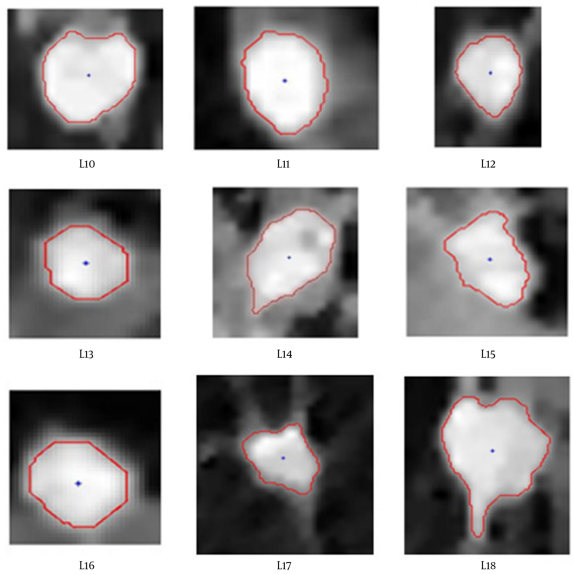

Figure 5. Extracted Malignant Mass Lesions and Their Depicted Contour Using Fuzzy C-Mean Segmentation Method

3.7. Feature Extraction

We extracted a couple of chaos and fractal features from breast tumor MR images. In addition to LLE, we calculated the mean value of each time series as a measure of tumor size. Also the variance of time series was calculated. The LLE was calculated as a measure of chaos in the extracted time series. We calculated the variance of Lyapunov exponents (VarLE) to obtain another TS feature and quantify the spread of Lyapunov exponents. Also, we utilized fractal analysis to extract significant fractal features

besides the time series descriptors.

For classification of benign and spiculated masses, we used roughness in the boundary of masses as one of the main fractal features. Spiculated masses have rough variation in boundaries whereas the benign masses are round and with smooth variation (13). Therefore, the variation of FDs in different scales was utilized to extract important information for classification. N2 as shown in Equation 4 describes the amount of changes in FDs in different scales with respect to the maximum number of FDs, which is measured on the smallest scale. This feature, especially in low scales, has the information of spiculation with high resolution (13).

$$N2 = 1 - \frac{NB}{Max\,(NB)} \quad (4)$$

Where NB indicates FDs of the boundary of the mass.

Another feature, used in the classification of different masses, was circularity of the mass. We proposed two circularity measures in this research, Circ and NonCirc. The former shows the circularity of tumor and the latter indicates the non-circularity of the mass. These features can be defined as Equations 5 and 6:

$$Circ = \frac{4\pi}{CL} \quad (5)$$

$$NonCirc = \frac{max\,(TS) - min\,(TS)}{Mean\,(TS)} \quad (6)$$

Where CL indicates the length of mass contour and TS is the extracted time series of mass contour. The mean value of TS indicates the average radius of the tumor and the difference between TS maximum and minimum can quantify the degree of deviation from the circular shape.

It should be noted that all the implementations of feature extraction process were performed on a 2.53-GHz laptop computer, with 4 GB random access memory, in the MATLAB 7.12.0.635 software environment (MathWorks, Inc).

3.8. Statistical Analysis

In this cross-sectional study we selected 18 samples using a systematic sampling method. We used Pierson's correlation analysis to present the significance of each parameter. Due to the small size of our database, it cannot have a normal distribution. We performed bootstrap method based on 5,000 bootstrap samples to solve the problem of small sample size. The obtained results are reported in Table 2.

3.9. Statistical Software

Statistical analysis was performed using the SPSS software for windows, version 19.0.0 (SPSS Inc., Chicago, IL).

This study was considered by the ethical committee of our university, and as it used available information of patients for regular diagnostic procedures, it was approved by this committee. We did not change any standard diagnostic procedure or imaging protocols.

4. Results and Discussion

The plot of Lyapunov exponents is depicted in Figure 6 for typical benign and malignant mass lesions. We extracted several chaotic, fractal and time series features and evaluated them by correlation analysis. Table 3 shows the extracted features and their values. In this malignant malignant and benign cases were coded with 1 and 0, respectively. As can be seen in Table 3, the LLE of all time series was positive. This fact indicates chaos in these time series. The majority of breast tumors had an irregular shape and ill-defined margin. We traced their contour according to the gray level values and concentration of contrast agent. The obtained results show that the degree of chaos in malignant cases was higher than benign cases, as expected. Table 2 shows positive and negative correlations with pathology results. According to this table, LLE and non-circularity with the correlation of 0.745 (P value = 0.000) and -0.494 (P value = 0.037) respectively, showed a higher correlation with pathology results in comparison with other features.

The low resolution of MRI, time delay, and embedding dimension estimation were our leading limitations in this research. One of the limitations of our study was that the results depended on the resolution of MR image. The higher the resolution, the more accurate extraction of chaos and fractal features. Also, the segmentation method plays an important role in the calculation of features. Accurate segmentation can lead to an accurate diagnosis using this method. It was difficult to segment breast tumors due to their vague and unclear margins. One of the strong points of our study was the use of fuzzy C-mean segmentation, which is fast and consistent. C-mean segmentation worked better than region growing methods on MRI images. Also, finding new significant features such as LLE, varLE and non-circularity were the other strong points of our study. This method is a non-invasive, quick, painless and non-radiational method (20), which can successfully help radiologists diagnose breast tumors more accurately, although it requires a larger database.

According to Table 3, if we choose a threshold of 0.17 just for LLE, we can correctly classify 17 out of 18 mass lesions. The only misclassified lesion was L1, which showed

Table 2. Bootstrap Analysis Based on 5000 Bootstrap Samples

	Pathology	LLE	N2	Mean	Var	varLE	circ1	noncirc
Pathology (Pierson's correlation)	1	0.745	-0.336	-0.307	-0.352	0.419	0.381	-0.494
P Value		0	0.172	0.215	0.152	0.083	0.119	0.037
Bootstrap								
Bias	0	0.035	0.002	0.009	-0.034	0.068	-0.002	0.009
Std. Error	0	0.089	0.211	0.203	0.133	0.138	0.201	0.184
95%Confidence Interval								
Lower	1	0.614	-0.695	-0.639	-0.647	0.249	-0.061	-0.822
Upper	1	0.943	0.118	0.160	-0.105	0.796	0.718	-0.094

Figure 6. Diagram of Lyapunov Exponents for A, a Benign and B, a Malignant Mass Lesion

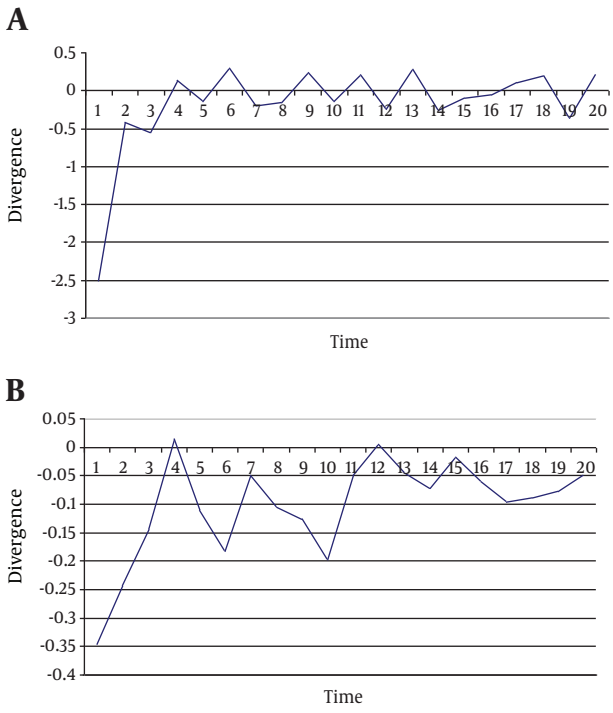

The slope of the first linear part of a curve fitted to these points was the LLE (19). This slope is higher in malignant tumors in comparison with benign ones.

a higher LLE in comparison with other benign patterns. This can be due to its larger size and segmentation errors. The second significant descriptor with Pearson's correlation of -0.494 was NonCirc. It showed the degree of non-circularity of the mass and as can be seen in Table 3, it had higher values in benign lesions. We can conclude that non-circular and long tumors are more likely to be benign rather than malignant. As indicated by Table 3, highest non-circularity index in L2, L3, L6 and L7 and all of these tumors was benign.

4.1. Conclusions

According to the obtained results, it can be concluded that the time series extracted from breast tumor margin showed chaotic behavior and can be described by a non-linear chaotic dynamical system. In order to measure the degree of chaos in time series of MR images, we computed the largest Lyapunov exponent using Rosenstein's method. We found that the value of LLE in malignant tumors was higher than benign mass lesions. This indicated a high Pearson's correlation of 0.745 (P value = 0.000) with pathology results. We can conclude that the LLE is one of the leading features in the early detection of breast cancer using dynamic MRI. Also, the variance of Lyapunov exponents (VarLE) was a significant feature in the prediction of malignancy. Moreover, we applied N2 as a fractal feature and NonCirc (P value = 0.037) on our dataset to evaluate the performance of fractal and time series features. These features were used to identify roughness of the mass contours, which is meaningful for radiologists in the diagnosis of spiculated masses. The obtained results indicate that non-circular and long tumors are more likely to be benign rather than malignant. Although the low resolution of MRI can reduce the accuracy of feature extraction, it can be improved by image processing solutions. Considering all limitations, LLE is still the best feature in comparison with other features. In conclusion, using non-linear dynamics and chaos to establish computer aided diagnosing models for early detection of breast cancer was a successful challenge.

Footnotes

Authors' Contribution: Study concept and design: Majid Pouladian and mahyar Nirouei; analysis and interpreta-

Table 3. The Extracted Chaos, Fractal and Time Series Features

Lesion	Pathology	LLE	N2	Mean	Var	varLE	Circ	NonCirc
1	0	0.2164	0.9953	27.3562	6.5244	0.2205	0.0744	0.4562
2	0	0.0558	0.9951	24.1196	54.0225	0.0429	0.0694	1.2947
3	0	0.0317	0.9941	21.0427	98.2916	0.0102	0.08	1.5356
4	0	0.0301	0.9893	12.1912	2.3557	0.2575	0.1721	0.4143
5	0	0.1575	0.9952	25.5841	7.6092	0.0982	0.0795	0.4176
6	0	0	0.9978	43.2796	324.1108	0	0.0373	1.5094
7	0	0.0534	0.9931	16.7414	40.9627	0.0807	0.1065	1.4756
8	0	0.0648	0.9916	15.0867	14.8594	0.1679	0.1102	0.9855
9	0	0.0646	0.9908	14.4089	11.0714	0.2442	0.1412	0.9625
10	1	0.4254	0.9931	20.8533	2.4596	0.3288	0.1022	0.3169
11	1	0.2594	0.9904	14.5141	4.5455	0.3891	0.1412	0.5103
12	1	0.8283	0.9897	12.661	0.9814	1.6171	0.1698	0.3091
13	1	0.3242	0.9897	11.5839	8.2113	0.3283	0.1904	0.8341
14	1	0.3412	0.9951	24.4411	23.2672	0.071	0.0816	0.7624
15	1	0.2549	0.9916	16.0728	11.1049	0.2858	0.1244	0.7386
16	1	0.1998	0.9874	11.1149	0.769	0.3616	0.1995	0.3151
17	1	0.3343	0.9939	20.1306	12.3159	0.2681	0.0967	0.6577
18	1	0.3416	0.9951	25.7149	29.5352	0.1013	0.0726	0.9397

tion of data: Mahyar Nirouei; drafting of the manuscript: Parviz Abdolmaleki and Mahyar Nirouei; critical revision of the manuscript for important intellectual content: Parviz Abdolmaleki and Mahyar Nirouei; statistical analysis: Mahyar Nirouei and Shahram Akhlaghpour; data Preparation: Shahram Akhlaghpour.

Conflict of Interest: The authors declare no conflicts of interest.

References

1. Lucht RE, Knopp MV, Brix G. Classification of signal-time curves from dynamic MR mammography by neural networks. *Magn Reson Imaging.* 2001;**19**(1):51–7. [PubMed: 11295347].
2. Collins DJ, Padhani AR. Dynamic magnetic resonance imaging of tumor perfusion. Approaches and biomedical challenges. *IEEE Eng Med Biol Mag.* 2004;**23**(5):65–83. [PubMed: 15565801].
3. Lee SH, Kim JH, Park JS, Chang JM, Park SJ, Jung YS, et al, editors. Texture analysis of lesion perfusion volumes in dynamic contrast-enhanced breast MRI. 2008 5th IEEE International Symposium on Biomedical Imaging: From Nano to Macro. 2008; IEEE; pp. 1545–8.
4. Tambasco M, Magliocco AM. Relationship between tumor grade and computed architectural complexity in breast cancer specimens. *Hum Pathol.* 2008;**39**(5):740–6. doi: 10.1016/j.humpath.2007.10.001. [PubMed: 18439940].
5. Dobrescu R, Ichim L, Crisan D. Diagnosis of breast cancer from mammograms by using fractal measures. *Int J Med Imag.* 2013;**1**(2):32–8.
6. Lopes R, Betrouni N. Fractal and multifractal analysis: a review. *Med Image Anal.* 2009;**13**(4):634–49. doi: 10.1016/j.media.2009.05.003. [PubMed: 19535282].
7. Louridas GE, Louridas AG. Impact of chaos in the progression of heart failure. *Int J Appl.* 2012;**2**(7).
8. EtehadTavakol M, Ng EYK, Lucas C, Sadri S, Ataei M. Nonlinear analysis using Lyapunov exponents in breast thermograms to identify abnormal lesions. *Infrared Phys Technol.* 2012;**55**(4):345–52.
9. Abe T, Chen Y, Pham TD. Biomed Inform Technol. Springer; 2014. pp. 257–70.Chaos Analysis of Brain MRI for Studying Mental Disorders.
10. Pham TD, Ichikawa K. Spatial chaos and complexity in the intracellular space of cancer and normal cells. *Theor Biol Med Model.* 2013;**10**:62. doi: 10.1186/1742-4682-10-62. [PubMed: 24152322].
11. Badas MG, Espa S, Fortini S, Querzoli G. 3D Finite Time Lyapunov Exponents in a left ventricle laboratory model. *EPJ Web Conferences.* 2015;**92**.
12. Rangayyan RM, Nguyen TM. Fractal analysis of contours of breast masses in mammograms. *J Digit Imaging.* 2007;**20**(3):223–37. doi: 10.1007/s10278-006-0860-9. [PubMed: 17021926].
13. Beheshti SM, AhmadiNoubari H, Fatemizadeh E, Khalili M. An efficient fractal method for detection and diagnosis of breast masses in mammograms. *J Digit Imaging.* 2014;**27**(5):661–9. doi: 10.1007/s10278-013-9654-z. [PubMed: 24777687].
14. Pineda FD, Medved M, Fan X, Ivancevic MK, Abe H, Shimauchi A, et al. Comparison of dynamic contrast-enhanced MRI parameters of breast lesions at 1.5 and 3.0 T: a pilot study. *Br J Radiol.* 2015;**88**(1049):20150021.
15. Gordillo N, Montseny E, Sobrevilla P. State of the art survey on MRI brain tumor segmentation. *Magn Reson Imaging.* 2013;**31**(8):1426–38. doi: 10.1016/j.mri.2013.05.002. [PubMed: 23790354].
16. Ertas G, Doran SJ, Leach MO. A computerized volumetric segmentation method applicable to multi-centre MRI data to support computer-aided breast tissue analysis, density assessment and lesion localization. *Med Biol Engineering Comput.* 2016:1–12.

17. Takens F. In: Lecture Notes in Mathematics. Rand DA, Young LS, editors. ; 1981. pp. 366–81.Detecting strange attractors in turbulence.
18. Rosenstein MT, Collins JJ, De Luca CJ. A practical method for calculating largest Lyapunov exponents from small data sets. *Physica D Nonlinear Phenomena*. 1993;**65**:117–34. doi: 10.1016/0167-2789(93)90009-p.
19. Pazo D, Lopez JM, Politi A. Diverging Fluctuations of the Lyapunov Exponents. *Phys Rev Lett*. 2016;**117**(3):034101. doi: 10.1103/PhysRevLett.117.034101. [PubMed: 27472112].
20. Ghayoumi Zadeh H, Haddadnia J, Montazeri A. A Model for Diagnosing Breast Cancerous Tissue from Thermal Images Using Active Contour and Lyapunov Exponent. *Iran J Public Health*. 2016;**45**(5):657–69. [PubMed: 27398339].